Editors' Suggestion

Invisible Gateway by Superscattering Effect of Metamaterials

Kang-Ping Ye,[1] Wen-Jin Pei,[1] Zhong-Hao Sa,[1] Huanyang Chen,[2,*] and Rui-Xin Wu[1,†]
[1]School of Electronic Science and Engineering, Nanjing University, Nanjing 210093, China
[2]Department of Physics and Institute of Electromagnetics and Acoustics, Xiamen University, Xiamen 361005, China

(Received 5 January 2021; accepted 12 May 2021; published 4 June 2021)

Illusion devices, such as superscatterer and invisible gateway, have been theoretically studied under the theory of transformation optics and folded geometry transformations. The realization of these devices needs building blocks of metamaterials with negative permittivities and permeabilities. However, superscattering effects, such as stopping wave propagation in an air channel, have not been verified from illusion devices physically because of the challenge of metamaterial design, fabrication, and material loss. In this Letter, we implement a big metamaterial superscatterer, and experimentally demonstrate its superscattering effect at microwave frequencies by field-mapping technology. We confirm that superscattering is originated from the excitation of surface plasmons. Integrated with superscatterer, we experimentally display that an invisible gateway could stop electromagnetic waves in an air channel with a width much larger than the cutoff width of the corresponding rectangular waveguide. Our results provide a first direct observation of superscattering effect of double negative metamaterials and invisible gateway for electromagnetic waves. It builds up an ideal platform for future designs of other illusion devices.

DOI: 10.1103/PhysRevLett.126.227403

Benefited from the powerful creativity of transformation optics [1–4], many abnormal applications, such as invisibility cloaks [5–9], electromagnetic (EM) field rotators [10,11], concentrators [12–14], and waveguide bends [15–19] are developed. Under the concept of complementary medium [20,21] and folding geometry transformation [22], transformation optics has been theoretically utilized to design illusion optical devices [23–26]. The key of these devices is the superscatterer whose scattering cross section is larger than its geometric size for observers of all directions [20]. The superscatterer has many interesting applications, such as superabsorber [25] and cloak at a distance [24]. To realize such a superscatterer requires a shell made of inhomogeneous and anisotropic negative refractive index metamaterial according to the complementary medium theory. Though different designs are theoretically proposed [27,28], there remain the difficulties of complicated constitutive parameters and material loss to be resolved. One improvement of the design is using uniform double negative metamaterial (DNM) [29] with a refractive index $n = -1$, which may ease the realization of the superscatterer. Meanwhile, all-dielectric metamaterials [30] is recently proposed to reduce the loss.

A fascinating application of the superscatterer is invisible EM gateway [29,31]. Such a gateway can stop the wave propagation in an air channel with a width much larger than the cutoff width of the corresponding rectangular waveguide. A proof-of-principle experiment of the invisible gateway was demonstrated by a circuit simulator [32]. It imitates the double negative materials and conventional materials by periodic inductor-capacitor networks, and the wave propagation in the gateway is mimicked by the voltage distribution on the networks. Though the experiment demonstrates the principle of the invisible gateway, to the best of our knowledge, there has been no report so far on discovering such superscattering effect and then implementing invisible gateway experimentally for EM waves in real time. It should be noted that the superscattering or strongly enhanced scattering of a subwavelength object could be achieved in certain directions simply by enhancing some orders of scattering [33–35]. However, the superscatterer here has to be the same scattering effect as that of its equivalent virtual object. Since the scattering field of an object can be expressed by a series of cylindrical waves in different orders in two dimensions, the same scattering effect indicates all orders of cylindrical waves for both the superscatterer and its equivalent virtual object should be the same. This is required for devices of illusion optics, so as to the application of invisible gateway [20,29].

In this work, we discover the superscattering effect experimentally from double-negative metamaterials made of self-biased ferrite rods in microwave X band. By using field-mapping technology, we experimentally show the metamaterial superscatterer can repel the incident radiation by the air in the mirror region of the superscatterer. We observe the electric field localized at the interface of air and DNM and decaying perpendicular to the interface, which confirms the theory of superscattering is related to the excitation of surface plasmons. By applying the superscatterer to implement the invisible gateway, we further experimentally demonstrate that the gateway can stop

incident waves in the air channel with a width much wider than the cutoff width of the corresponding waveguide. Our study provides real observation of the superscattering effect of double negative metamaterials and the invisible gateway for EM waves.

Superscatterer by double-negative metamaterials.—We consider the superscattering of TE waves (with electric field along the z axis) from a scatterer in the air background as shown in Fig. 1(a). The scatterer is an all-dielectric metamaterial with partial boundaries covered by a layer of metal (in gray), which acts as a perfect electric conductor (PEC) boundary. The metamaterial is composed of self-biased Sr-ferrite rods arranged in a hexagonal lattice (a magnetic photonic crystal, PC) [36,37]. Theoretical results predict that its effective relative permittivity ε_r and permeability μ_r are simultaneously negative one at the frequency of 10.8 GHz (Supplemental Material [38], Fig. S1).

It is known that any medium will be optically canceled by the material constructed to be an inverted mirror image of the medium with ε_r and μ_r reversed in sign [21]. Particularly, if the material parameters are $\varepsilon_r = \mu_r = -1$,

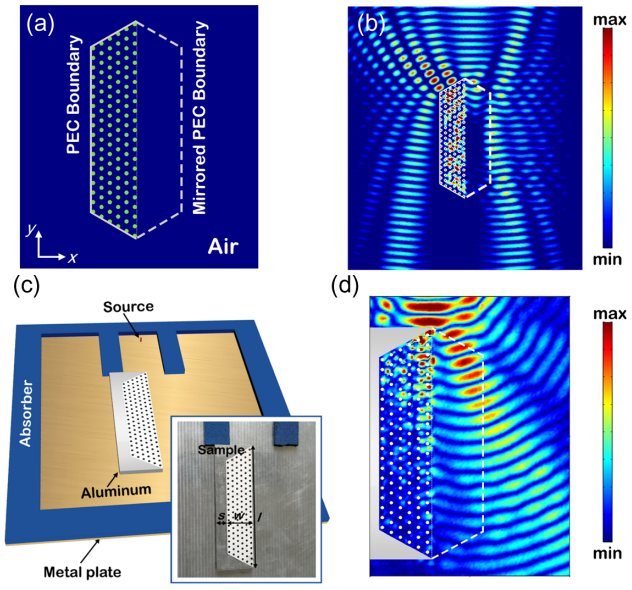

FIG. 1. Superscattering effect of PC metamaterial. (a) Schematic of the superscatterer. Ferrite rods (green dots) in air (blue background) is partially enclosed by PEC (in gray). The dash line is the virtual boundary of the mirror image of the PEC. The radius of the rods is 2 mm and the lattice constant is 10 mm. (b) Superscattering effect at 10.6 GHz in simulation. The incident plane wave is repelled away from the air within the dash lines. (c) Schematic of the experimental setup for the superscatterer. The inset is the local view of the sample. The size of the metamaterial block is $w = 51$ mm, $l = 235$ mm, and the sharp angle is 60°. The width of metal block is $s = 21$ mm. The waveguide constructed by two absorbers is to generate incident plane wave. (d) The measured electric field E_z around the sample at 10.38 GHz. The ferrite rods are marked in white dots and aluminum is in gray.

the metamaterial scatterer and its mirror image in the air form a pair of complementary media where the phase accumulated in the metamaterial is exactly canceled by the air [21]. As a result, in Fig. 1(a), the PEC boundary will be mapped to the virtual PEC boundary in the air marked in a dashed line, resulting in an equivalent bigger metallic block that includes both the metamaterial and its mirror image. The scatterer becomes a superscatterer with an increased scattering cross section for the far-field observers. We simulate the response of the superscatterer illuminated by a plane wave under normal incidence. Simulations in this Letter are carried out in COMSOL MULTIPHYSICS. Different from the reported superscatters [33,34], here the scatterer is with the feature size over the working wavelength. Figure 1(b) shows the electric field distribution near the superscatterer when a plane wave radiates from the top. We see that the EM wave bounced away from the virtual PEC boundary. The phenomenon clearly indicates that the incident wave experiences a scatterer whose electric size is bigger than its physical size. The physics behind such superscattering effect is related to the excitation of surface plasmons at the interface of the metamaterial and air [29], where the evanescent waves are amplified [4]. The calculations show that the strongest superscattering happens at the frequency of about 10.6 GHz, slightly different from the theoretical frequency of index $n_{\text{eff}} = -1$. The reason may be the lattice-induced anisotropy of the magnetic PC metamaterial.

Experimental verification of supperscattering effect.—We implemented the double negative PC metamaterial by embedding self-biased Sr-ferrite rods in the acrylonitrile butadiene styrene background material engineered by 3D printing technology (Supplemental Material [38], Sec. I). Refractive experiments proved the effective index of the PC metamaterial is $n_{\text{eff}} \approx -1$ near the frequency of 10.66 GHz (Supplemental Material [38], Fig. S2) at which the material loss is low [37]. The superscatterer was fabricated by a trapezoidal PC metamaterial and a metal block. Figure 1(c) shows the superscatterer in the experimental setup which is in the size of $w = 51$ mm, $l = 235$ mm, and the vertex angle is 60° (not marked in the figure). The metal block splice to the metamaterial functions as the PEC boundary. In experiments, the plane wave was formed by the waveguide assembled by two absorbers with a gap of 90 mm. A microwave field-mapping device was used to characterize the response of the superscatterer (Supplemental Material [38], Sec. VI).

Figure 1(d) illustrates the experimental result. In the figure, the Sr rods are marked in white dots and the aluminum block is in gray. We can see the incident plane wave is pushed away from the air in the mirror area of the metamaterial. Further, we observe the surface plasmons excited at the interface of metamaterial and air; where the electric field concentrates on the interface of PC metamaterial and decays perpendicular to the interface, which

confirms the superscatterer is related to surface plasmons. Because of the inevitably material loss, the superscattering phenomenon is not so evident as the lossless case shown in Fig. 1(b). The incident field may infiltrate into the virtual PEC boundary, and the surface plasmons decay along with the interface. A more detailed discussion can be found in the Supplemental Material [38]. These observations are the first time for the superscattering effect to be confirmed in experiments.

We note the strongest superscattering effect appears at the frequency of 10.38 GHz, which slightly deviates from that of the index $n = -1$ in the refraction experiment. The frequency shift contributed by somewhat inevitable anisotropy of the PC metamaterial, also appears in the simulations.

Invisible gateway by superscatterer.—Figure 2(a) displays the schematic of the gateway made of the superscatterer and the metal blocks (in gray). The metal block on the right locates exactly at the position where the virtual PEC boundary is [see Fig. 1(a)]. This indicates the electrical width of the air channel is zero and the channel will virtually be blocked. Consequently, the gateway seems to be invisible for the incident wave (the invisible gateway). As a demonstration, Fig. 2(b) plots the wave propagation in the gateway. The incident wave is excited by a line current source at the top of the channel and on the centerline of the gateway. The figure shows the incident wave is trapped in the gateway and inhibited going through the channel. The incident wave will not "see" the gateway. In contrast, if the metamaterial is replaced by a metal, the wave can pass through the gateway as shown in Fig. 2(c). In this case, the gateway can be considered as a rectangular waveguide working in TE_{10} mode. Its cutoff wavelength is about 95 mm, which is much larger than the working wavelength (about 28 mm). Thus, the gateway opens and can be seen for the incident wave.

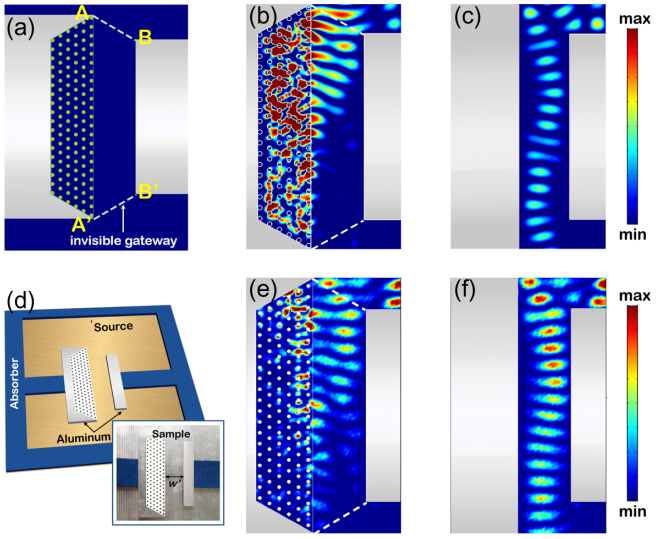

FIG. 2. Invisible gateway of PC metamaterial. (a) Schematic of the invisible gateway formed by the superscatterer and a metal block on the right side. (b),(c) the electric field distribution in the invisible gateway and PEC waveguide, respectively, simulated at 10.6 GHz. (d) Schematic of experimental setup for the invisible gateway. The inset is the sample image of the gateway with $w' = 51$ mm, the same as the width of the PC metamaterial sample. (e) Measured electric field distribution in the invisible gateway. The wave is stopped in the gateway. The surface plasmons appear on the interface of the metamaterial and the air. (f) Measured electric field when the metamaterial is replaced by a metal. The wave goes through the gateway without decay. All measurements were performed at 10.38 GHz.

Though the cutoff waveguide can stop the incident wave, the invisible gateway stops the waves in a much wider air channel. Generally, the cutoff waveguide forbids wave propagation when the working wavelength λ is greater than the cutoff wavelength of a waveguide. This requires the width of the waveguide to be less than 0.5 λ for the rectangular waveguides working in TE_{10} mode. However, for the invisible gateway mentioned above, the width is about 1.7 λ, which is much larger than that of the conventional cutoff waveguide.

Experimental verification of invisible gateway.—We implemented an invisible gateway as schematically displayed in Fig. 2(d). The air channel between the superscatterer and the metal block is $w' = 51$ mm, the same as the width of the PC metamaterial. A line current source, about 100 mm above the gateway, is used to excite EM waves. The absorbers on the two sides of the gateway absorb the incident radiation to avoid the interference of the incident wave to the measurements.

Figure 2(e) shows the result of the field-mapping measurement. We see the incident radiation penetrates the gateway and attenuates rapidly along the channel. At the end of the air channel, the field almost decays away. The experimental result is in good agreement with the simulation one displayed in Fig. 2(b), which confirms the invisible gateway is caused by the superscattering effect of the PC metamaterial. As a comparison, Fig. 2(f) shows the experiment result where the metamaterial is replaced by a metallic object. In this case, the incident radiation penetrates the gateway and goes through the gateway without attenuation. We compute and compare the electric field energy density (EED) averaged over the ports of the gateway (Supplemental Material [38], Sec. III) since the field-mapping technology only records the electric field. The ratio of the EED at the output port [line $A'B'$ in Fig. 2(a)] to the input port (line AB) is -10 dB. For the metal waveguide the ratio is about -2.5 dB.

To show how the invisible gateway stops the wave propagation, we plot the EED in the gateway, which is displayed in Fig. 3(a). In the gateway along the direction from position B to B', the EED decay rapidly. At position B', the EED is only 10% of that of position B; 90% of the energy is blocked. Here, the EED is averaged over the cross section of the air channel. In contrast, the behavior of wave

in the metal waveguide is much smoother and the EED attenuation is only about 15%. The results are consistent with the data obtained by simulations, which are shown in lines.

Discussions.—The effective index of our PC metamaterial is frequency dispersive. The deviation of the index from $n = -1$ and the loss of the metamaterial will weaken the superscattering effects. Nevertheless, we find the invisible gateway can still work in a certain frequency range. The simulations show that the invisible gateway is more sensitive to the effective refractive index away from $n = -1$ than the loss (Supplemental Material [38], Fig. S6). When the refractive index of the metamaterial is between -0.93 and -1.07, the gateway can still stop the wave propagation (Supplemental Material [38], Fig. S7).

Figure 3(b) shows the frequency dependence of EED ratio at the two ports for the experiment. The ratio goes to a minimum of about -10 dB at 10.38 GHz. The small energy leakage is mainly caused by the somewhat anisotropy of the PC metamaterial DNM. The leakage will grow fast if the frequency deviates a little. Indeed, in experiments we observed the gateway forbids the wave propagation somewhat with a narrow frequency range, but the field patterns are not so good as displayed in Fig. 2(e). If the invisible gateway includes a uniform DNM, there will be little leakage (Supplemental Material [38], Fig. S6). At the frequencies of 10.35 and 10.43 GHz, the ratios are -7 and -8 dB, respectively, where we observed the field pattern that stops wave propagation somewhat (Supplemental Material [38], Fig. S8).

Furthermore, in magnetized states ferrite's permeability depends on bias magnetic field, therefore the effective index of metamaterial can be tuned by the bias magnetic field. This provides a special advantage for the currently invisible gateway; at a given frequency we can switch the gateway in the states of visible or invisible in real time by tuning the external bias field, or change the working frequency of the invisible gateway as required (Supplemental Material [38], Secs. 4 and 5). Such advantages are also available for the metamaterial fabricated by other tunable materials, such as phase change materials [43].

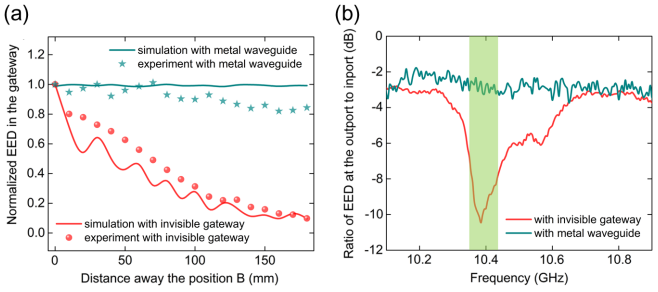

FIG. 3. Averaged electric field energy density in the gateway. (a) The electric field energy density along the air channel of the invisible gateway and metal waveguide, respectively. (b) Frequency dependence of measured ratio of electric field energy density at the output port to the input port for the invisible gateway and metal waveguide. The minimum ratio happens at 10.38 GHz. Deviating from the frequency of the minimum, the invisible gateway shows a weakened but visible phenomenon of stopping wave propagation in the air channel in the shadowed frequency interval.

In summary, we have implemented a superscatterer at microwave frequencies by a double negative metamaterial fabricated by self-biased ferrite rods. Using field-mapping technology, we experimentally verify the physics of the superscattering effect for EM waves: the incident plane wave is repelled by the surface plasmons at the interface of air and DNM. The superscatterer is then applied to the invisible gateway, where we show that it can stop the wave propagation in the air channel whose width is much larger than the cutoff value of the corresponding waveguide. Our results provide direct observation of the superscattering effect of double negative metamaterials and the invisible gateway for electromagnetic waves. The index tunability of magnetic PC metamaterial can make the invisible gateway switchable and tunable. Our implementation provide an ideal platform for future designs of illusion devices that are a fascinating research field in transformation optics [44].

This work was supported by National Natural Science Foundation of China (NSFC) (61771237), and partially by the Project funded by the Priority Academic Program Development of Jiangsu Higher Education Institutions and Jiangsu Provincial Key Laboratory of Advanced Manipulating Technique of Electromagnetic Waves. H. C. was supported by the National Science Foundation of China (Grant No. 11874311) and would like to celebrate the centennial anniversary of Xiamen University.

*Corresponding author.
kenyon@xmu.edu.cn
†Corresponding author.
rxwu@nju.edu.cn

[1] U. Leonhardt, Optical conformal mapping, Science **312**, 1777 (2006).
[2] J. B. Pendry, D. Schurig, and D. R. Smith, Controlling electromagnetic fields, Science **312**, 1780 (2006).
[3] V. M. Shalaev, Transforming light, Science **322**, 384 (2008).
[4] H. Y. Chen, C. T. Chan, and P. Sheng, Transformation optics and metamaterials, Nat. Mater. **9**, 387 (2010).
[5] D. Schurig, J. J. Mock, B. J. Justice, S. A. Cummer, J. B. Pendry, A. F. Starr, and D. R. Smith, Metamaterial electromagnetic cloak at microwave frequencies, Science **314**, 977 (2006).
[6] J. Li and J. B. Pendry, Hiding under the Carpet: A New Strategy for Cloaking, Phys. Rev. Lett. **101**, 203901 (2008).
[7] R. Liu, C. Ji, J. J. Mock, J. Y. Chin, T. J. Cui, and D. R. Smith, Broadband ground-plane cloak, Science **323**, 366 (2009).

[8] J. Valentine, J. S. Li, T. Zentgraf, G. Bartal, and X. Zhang, An optical cloak made of dielectrics, Nat. Mater. **8**, 568 (2009).

[9] L. H. Gabrielli, J. Cardenas, C. B. Poitras, and M. Lipson, Silicon nanostructure cloak operating at optical frequencies, Nat. Photonics **3**, 461 (2009).

[10] H. Y. Chen and C. T. Chan, Transformation media that rotate electromagnetic fields, Appl. Phys. Lett. **90**, 241105 (2007).

[11] H. Y. Chen, B. Hou, S. Y. Chen, X. Y. Ao, W. J. Wen, and C. T. Chan, Design and Experimental Realization of a Broadband Transformation Media Field Rotator at Microwave Frequencies, Phys. Rev. Lett. **102**, 183903 (2009).

[12] M. Rahm, D. Schurig, D. A. Roberts, S. A. Cummer, D. R. Smith, and J. B. Pendry, Design of electromagnetic cloaks and concentrators using form-invariant coordinate transformations of Maxwell's equation, Photonics Nanostruct. Fundam. Appl. **6**, 87 (2008).

[13] W. X. Jiang, T. J. Cui, Q. Cheng, J. Y. Chin, X. M. Yang, R. P. Liu, and D. R. Smith, Design of arbitrarily shaped concentrators based on conformally optical transformation of nonuniform rational *B*-spline surfaces, Appl. Phys. Lett. **92**, 264101 (2008).

[14] M. M. Sadeghi, S. C. Li, L. Xu, B. Hou, and H. Y. Chen, Transformation optics with Fabry-Pérot resonances, Sci. Rep. **5**, 8680 (2015).

[15] J. T. Huangfu, S. Xi, F. M. Kong, J. J. Zhang, H. S. Chen, D. X. Wang, B. Wu, L. X. Ran, and J. A. Kong, Application of coordinate transformation in bent waveguides, J. Appl. Phys. **104**, 014502 (2008).

[16] D. A. Roberts, M. Rahm, J. B. Pendry, and D. R. Smith, Transformation-optical design of sharp waveguide bends and corners, Appl. Phys. Lett. **93**, 251111 (2008).

[17] W. X. Jiang, T. J. Cui, X. Y. Zhou, X. M. Yang, and Q. Cheng, Arbitrary bending of electromagnetic waves using realizable inhomogeneous and anisotropic materials, Phys. Rev. E **78**, 066607 (2008).

[18] P.-H. Tichit, S. N. Burokur, and de A.Lustrac, Waveguide taper engineering using coordinate transformation technology, Opt. Express **18**, 767 (2010).

[19] T. Han, C.-W. Qiu, and X. Tang, Adaptive waveguide bends with homogeneous, nonmagnetic, and isotropic materials, Opt. Lett. **36**, 181 (2011).

[20] T. Yang, H. Chen, X. Luo, and H. Ma, Superscatterer: Enhancement of scattering with complementary media, Opt. Express **16**, 18545 (2008).

[21] J. B. Pendry and S. A. Ramakrishna, Focusing light using negative refraction, J. Phys. **15**, 6345 (2003).

[22] G. W. Milton, N. A. P. Nicorovici, R. C. McPhedran, K. Cherednichenko, and Z. Jacob, Solutions in folded geometries, and associated cloaking due to anomalous resonance, New J. Phys. **10**, 115021 (2008).

[23] Y. Lai, J. Ng, H. Y. Chen, D. Z. Han, J. J. Xiao, Z. Q. Zhang, and C. T. Chan, Illusion Optics: The Optical Transformation of an Object into Another Object, Phys. Rev. Lett. **102**, 253902 (2009).

[24] Y. Lai, H. Y. Chen, Z.-Q. Zhang, and C. T. Chan, Complementary Media Invisibility Cloak that Cloaks Objects at a Distance Outside the Cloaking Shell, Phys. Rev. Lett. **102**, 093901 (2009).

[25] J. Ng, H. Y. Chen, and C. T. Chan, Metamaterial frequency-selective superabsorber, Opt. Lett. **34**, 644 (2009).

[26] W. Li, J. G. Guan, W. Wang, Z. G. Sun, and Z. Y. Fu, A general cloak to shift the scattering of different objects, J. Phys. D **43**, 245102 (2010).

[27] X. Zang and C. Jiang, Two-dimensional elliptical electromagnetic superscatterer and superabsorber, Opt. Express **18**, 6891 (2010).

[28] C. Yang, J. Yang, M. Huang, J. Peng, and G. Cai, Two-dimensional electromagnetic superscatterer with arbitrary geometries, Comput. Mater. Sci. **49**, 820 (2010).

[29] H. Y. Chen, C. T. Chan, S. Liu, and Z. A. Lin, Simple route to a tunable electromagnetic gateway, New J. Phys. **11**, 083012 (2009).

[30] S. Jahani and Z. Jacob, All-dielectric metamaterials, Nat. Nanotechnol. **11**, 23 (2016).

[31] X. D. Luo, T. Yang, Y. W. Gu, H. Y. Chen, and H. R. Ma, Conceal an entrance by means of superscatterer, Appl. Phys. Lett. **94**, 223513 (2009).

[32] C. Li, X. K. Meng, X. Liu, F. Li, G. Y. Fang, H. Y. Chen, and C. T. Chan, Experimental Realization of a Circuit-Based Broadband Illusion-Optics Analogue, Phys. Rev. Lett. **105**, 233906 (2010).

[33] Z. Ruan and S. Fan, Superscattering of Light from Subwavelength Nanostructures, Phys. Rev. Lett. **105**, 013901 (2010).

[34] C. Qian, X. Liu, Y. Yang, X. Y. Xiong, H. P. Wang, E. P. Li, I. Kaminer, B. L. Zhang, and H. S. Chen, Experimental Observation of Superscattering, Phys. Rev. Lett. **122**, 063901 (2019).

[35] C. Wang, C. Qian, H. Hu, L. Shen, Z. Wang, H. Wang, Z. Xu, B. Zhang, H. Chen, and X. Lin, Superscattering of light in refractive index near zero environments, Prog. Electromagn. Res. **168**, 15 (2020).

[36] S. Y. Liu, W. K. Chen, J. J. Du, Z. F. Lin, S. T. Chui, and C. T. Chan, Manipulating Negative-Refractive Behavior with a Magnetic Field, Phys. Rev. Lett. **101**, 157407 (2008).

[37] Y. Gu, R-X. Wu, Y. Yang, Y. Poo, P. Chen, and Z. F. Lin, Self-biased magnetic left-handed material, Appl. Phys. Lett. **102**, 231914 (2013).

[38] See Supplemental Material at http://link.aps.org/supplemental/10.1103/PhysRevLett.126.227403 for more information, which includes Refs. [39–42].

[39] S. A. Oliver, P. Shi, W. Hu, H. How, S. W. McKnight, N. E. McGruer, P. M. Zavracky, and C. Vittoria, Integrated self-biased hexaferrite microstrip circulators for millimeter-wavelength applications, IEEE Trans. Microwave Theory Tech. **49**, 385 (2001).

[40] D. M. Pozar, *Microwave Engineering*, 3rd ed. (Wiley, New York, 2005).

[41] Y. Wu, J. Li, Z.-Q. Zhang, and C. T. Chan, Effective medium theory for magnetodielectric composites: Beyond the long-wavelength limit, Phys. Rev. B **74**, 085111 (2006).

[42] J. F. Jin, S. Y. Liu, Z. F. Lin, and S. T. Chui, Effective-medium theory for anisotropic magnetic metamaterials, Phys. Rev. B **80**, 115101 (2009).

[43] P. Hosseini, C. D. Wright, and H. Bhaskaran, An optoelectronic framework enabled by low-dimensional phase-change films, Nature (London) **511**, 206 (2014).

[44] M. McCall, J. B. Pendry, V. Galdi *et al.* Roadmap on transformation optics, J. Opt. **20**, 063001 (2018).